Academic Journal of Science and Technology
ISSN: 2771-3032 | Vol. 21, No. 1, 2026

Spatiotemporal Dynamics of Cropland Non-agriculturalization in Zhengzhou City Using Deep Learning-Based Interpretation

Yaqing Zheng[1, *], Xiaoping Lu[1], Guosheng Cai[1]

[1]Key Laboratory of Spatio-Temporal Information and Ecological Restoration of Mines of Natural Resources of the People's Republic of China, Henan Polytechnic University, Jiaozuo 454003, China

[*] Correspondence: archie_z@qq.com

Abstract: Traditional monitoring of cropland non-agriculturalization heavily relies on land use/cover change data, which is constrained by long update cycles and the difficulty of accurately isolating the unidirectional conversion from cropland to non-agricultural uses. To address these limitations, this study utilizes a semantic change detection network with GaoFen-2 (GF-2) high-resolution time-series remote sensing imagery of Zhengzhou City from 2021 to 2025 as the primary data source. Integrating a land-use transfer matrix, grid cell analysis, spatial autocorrelation analysis, and the Geographic Detector model, we systematically analyze the spatiotemporal evolution dynamics and driving mechanisms of cropland non-agriculturalization in the region. The results demonstrate that: (1) Temporally, the intensity of cropland conversion in Zhengzhou City exhibits an unbalanced fluctuating pattern characterized by "initial intensity, subsequent stabilization, and localized rebound," with construction land being the absolute dominant destination of cropland outflow, resulting in a cumulative converted area exceeding 80 km² over the five-year period. (2) Spatially, cropland non-agriculturalization exhibits a distinct gradient pattern described as "commencing in the central urban core, highly aggregating in near suburbs, and dispersedly distributing with low intensity in far suburbs." Hot spot zones are heavily clustered in the near-suburb plains (e.g., Zhongmu County and Xinzheng City), whereas cold spot zones remain long-term stable in the western and southern hilly and mountainous regions (e.g., Dengfeng and Xinmi). The Global Moran's I indices are consistently positive and statistically significant, revealing pronounced spatial polarization and clustering features. (3) Regarding the driving mechanisms, cropland non-agriculturalization in Zhengzhou City is generally characterized by "transportation location dominance, industrial economic support, and topographical constraints."

Keywords: Land use; Non-agriculturalization of Cropland; Spatiotemporal Evolution.

1. Introduction

Fundamentally, cropland conversion is an objective reflection of macro-socioeconomic transformation and urban-rural spatial restructuring within land use dynamics. Accurately monitoring the spatiotemporal distribution characteristics of cropland non-agriculturalization not only objectively quantifies agricultural land loss but also provides solid scientific evidence and data support for regional territorial spatial management, strict adherence to the cultivated land protection red line, and the optimization of land resource allocation.

Early studies predominantly relied on mathematical and statistical analysis methods to explore the spatiotemporal characteristics of cropland non-agriculturalization based on long-term time series. These studies often approached the issue from the perspective of quantitative relationships between cropland non-agriculturalization and various elements of socioeconomic development systems at macro and meso scales in rapidly developing regions. For instance, using Wuhan City as the study area, Cai et al. [1] revealed the evolutionary pattern wherein non-agriculturalization hot spots cluster toward new urban districts and near-suburb zones. They also highlighted the significant spatial heterogeneity between core urban areas and near suburbs regarding construction land types (e.g., urban expansion versus industrial, mining, and transportation). In the dimension of macro-policy response, Zhong et al. [2] demonstrated through assessments in the southeastern hilly regions that the trajectories of cropland loss exhibit high spatiotemporal complexity. They found that national-level land-use regulations and strict redline policies constitute a substantial dampening effect that curbs the reduction rate of agricultural land. Additionally, focusing on the major agricultural producing areas in the Central Plains, Fan et al. [3] systematically reconstructed the non-agriculturalization flux and evolutionary characteristics across four major river basins in Henan Province at the county scale. They explicitly pointed out that surface morphology and baseline area act as the underlying physical constraints reshaping the spatial pattern of regional cropland.

With the development and application of GIS technology, researchers have increasingly combined land use data with spatial analysis tools to explore the spatial patterns of cropland non-agriculturalization. Based on land use data, Zhang et al. [4] utilized the spatial statistics and spatial analysis functions of ArcGIS to fit the spatial diffusion trajectories of cropland non-agriculturalization in Wuhan City. Ma et al. [5] conducted a quantitative analysis of the theoretical thresholds and empirical representations of construction land, thereby revealing the spatiotemporal differentiation pattern of agricultural land loss stress in Hubei Province; their study further introduced a center-of-gravity trajectory evolution algorithm to accurately reconstruct the dynamic migration characteristics of regional non-agriculturalization pressure. Based on land use and DEM data,

Qu et al. [6] employed methods such as mathematical statistics and spatial analysis to investigate the spatial pattern of cropland changes at the patch scale, indicating that the spatial dynamics of cropland conversion in Fujian Province from 1990 to 2015 exhibited a high-in-the-east and low-in-the-west pattern.

Focusing on 23 county-level areas across three border prefecture-level cities in Guangxi, Liu et al. [7] characterized the speed and direction of cropland non-agriculturalization from 1980 to 2018 by constructing center-of-gravity and standard deviational ellipse (SDE) models, and analyzed its spatial features using spatial autocorrelation analysis. Similarly, Huang et al. [8] applied the cropland non-agriculturalization center-of-gravity migration model and spatial autocorrelation analysis to explore the spatiotemporal evolution characteristics of cropland non-agriculturalization across 111 county-level evaluation units in Guangxi over the past 40 years. Using LUCC data, Li et al. [9] conducted research employing methods such as kernel density estimation (KDE) and the Geographic Detector model, revealing that cropland non-agriculturalization in Yan'an City predominantly occurs in areas with low slopes, medium elevations, and low topographic position indices (TPI). Wu et al. [10] investigated the cropland non-agriculturalization process and spatial distribution relationships at the county scale in Anhui Province, utilizing LUCC data, GIS spatial analysis tools, and drawing on the center-of-gravity migration model.

Furthermore, Li et al. [11] employed hot spot analysis, the SDE method, and center-of-gravity migration analysis based on land use data to reveal the spatiotemporal distribution patterns, site characteristics, and evolutionary trends of cropland non-agriculturalization in Yunnan Province over the past 30 years. Liu et al. [12] revealed the characteristics and evolutionary trends of cropland non-agriculturalization in the Lower Liaohe River Plain by combining land use data with ArcGIS spatial analysis. At the county scale, Liu et al. [13] adopted the exploratory spatial data analysis (ESDA) method to study the spatiotemporal evolution characteristics of cropland non-agriculturalization. Based on long-time-series land use spatial data of Henan Province from 1980 to 2020, Yu et al. [14] quantitatively revealed the spatial distribution characteristics, spatiotemporal migration paths, and agglomeration features of cropland non-agriculturalization across 158 county-level evaluation units using the center-of-gravity migration model and spatial autocorrelation analysis. Kang et al. [15] applied ArcGIS spatial overlay analysis and statistical tools to analyze the cropland non-agriculturalization process and spatial distribution characteristics across various townships in Danjiangkou City, showing that cropland in this city is primarily concentrated in the northern region. Finally, Li et al. [16] systematically explored the spatiotemporal evolution characteristics of cropland non-agriculturalization in the Jialing River Basin from 1980 to 2020 using the center-of-gravity migration model, ESDA, a land-use transfer matrix, and ArcGIS spatial overlay analysis. Their findings demonstrated spatial agglomeration of cropland non-agriculturalization, forming a stable pattern with the central basin acting as hot spot zones and the southern and eastern mountainous areas functioning as cold spot zones.

At present, studies analyzing the spatiotemporal distribution characteristics of cropland non-agriculturalization predominantly rely on existing land use/cover change (LUCC) datasets. However, practical monitoring of non-agriculturalization often demands high timeliness, requiring updates at a quarterly or even higher frequency. Consequently, the long update cycles of available data products struggle to meet these practical requirements. Furthermore, although a few scholars [17] have attempted to conduct independent monitoring using remote sensing image classification techniques, their classification results typically present only the net changes between cropland inflow and outflow. Because these classification maps inherently encompass the conversion processes of other land cover types into cropland, it remains challenging to directly and intuitively isolate and characterize the unidirectional conversion from cropland to non-agricultural uses.

2. Methods

In this paper, a semantic change detection model is introduced and combined with a land-use transfer matrix, grid cell analysis, and spatial autocorrelation analysis (Moran's I) to dissect the spatiotemporal characteristics of cropland non-agriculturalization in the study area. Furthermore, the driving mechanisms of this non-agriculturalization process are explored using the Geographic Detector model.

2.1. Deep Learning-Based Interpretation

To effectively address the semantic change detection (SCD) task in complex scenarios and simultaneously extract high-precision land-cover evolution boundaries and categorical attributes, this study designs an overall framework of an end-to-end multi-task learning network, with reference to [18] (as illustrated in Figure 1). The core of this architecture consists of three jointly optimized sub-networks: two semantic segmentation (SS) branches based on Siamese weight-sharing and one binary change detection branch. Notably, the weight-sharing strategy of the SS branches not only effectively controls the parameter size of the model but, more importantly, ensures the absolute consistency of the mapping space for feature extraction from the bi-temporal imagery.

At the network topology level, all three branches strictly follow the classical "encoder-decoder" paradigm to achieve the progressive recovery from high-level semantics to low-level spatial details. Addressing the variable scales and complex morphological characteristics of target objects such as cropland, this study introduces a multi-scale semantic segmentation module into the decoder stage of the SCD network. This module dynamically aggregates contextual information across multiple receptive fields without significantly increasing computational complexity, thereby substantially enhancing the network's fine-grained perception capability for changed regions of varying scales.

Furthermore, in terms of temporal feature modeling, considering that land-cover evolution in real-world scenarios typically follows specific spatiotemporal logic, the architecture introduces a graph learning-based temporal interaction module. By constructing topological node connections across cross-temporal features, this module models the long-range dependencies between the bi-temporal images. Consequently, it strongly enforces the semantic consistency of the SCD prediction results at the feature level, significantly reducing logical contradictions caused by complex environmental interference.

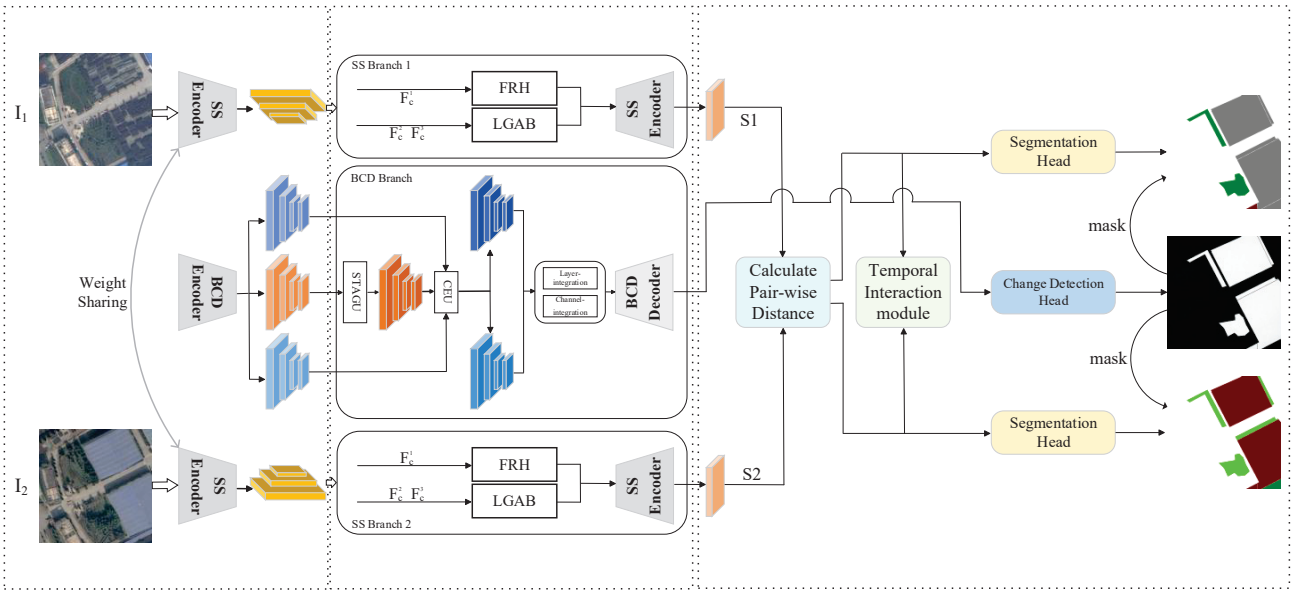

Figure 1. Architecture of the MCC-SCNet

After acquiring and preprocessing the bi-temporal high-resolution remote sensing imagery of the study area, this study constructs an end-to-end automated interpretation technological framework of "data input-model inference-spatial reconstruction" to accurately extract the spatiotemporal evolution features of cropland non-agriculturalization. The specific implementation steps are as follows:

(1) To overcome the GPU memory constraints of deep learning models regarding input image size while maximally preserving the local spatial contextual information of ground objects, this study employs a regular sliding window strategy with a predetermined overlap ratio. The massive bi-temporal remote sensing images are cropped into standard patch arrays of 256 × 256 pixels. Subsequently, the corresponding bi-temporal patch pairs are fed in batches into the trained and converged Multi-Channel Complementary Semantic Change Detection Network (MCC-SCNet) for forward inference, thereby generating patch-level, pixel-wise semantic prediction masks of cropland non-agriculturalization.

(2) Targeting the discrete predicted patches output by the model, seamless mosaicking and stitching based on coordinate mapping are executed, strictly relying on the original imagery's spatial reference system and geographic projection parameters. To eliminate edge gaps or artifact effects that may arise during the image cropping and stitching process, weighted fusion processing is applied to the predicted probabilities in the overlapping regions, ultimately achieving a high-fidelity reconstruction of the spatial distribution map of cropland non-agriculturalization evolution covering the entire study area.

(3) The aforementioned full-region interpretation results are imported into the ArcGIS platform, where scale conversion and spatial geometric calculations are performed based on the actual physical ground resolution of the raster pixels. On this basis, not only are the total converted area of cropland and the internal structural proportions of its conversion to various non-agricultural construction lands accurately calculated, but spatial overlay and topological analysis tools are also utilized to deeply characterize the spatial agglomeration features, expansion directions, and regional differentiation patterns of cropland non-agriculturalization. This provides solid data support for the subsequent exploration of driving mechanisms.

2.2. Spatiotemporal Distribution Analysis

To comprehensively dissect the spatiotemporal evolution characteristics of cropland non-agriculturalization in the study area from multiple dimensions, this section designs a comprehensive quantitative analysis framework structured around "conversion structure-evolution intensity-spatial pattern":

First, a land-use transfer matrix [19] is employed to accurately track the trajectories and scale of cropland conversion to various non-agricultural land types, thereby elucidating the structural characteristics of the non-agriculturalization evolution. Second, the grid cell spatial measurement method [17] is introduced for quantitative analysis; by constructing standardized spatial grids to calculate the non-agriculturalization index, this approach effectively mitigates the interference of administrative boundaries on the expression of spatial heterogeneity. Finally, exploratory spatial data analysis (ESDA) [20] is applied to examine the spatial autocorrelation of the cropland non-agriculturalization evolution, systematically exploring its spatial agglomeration and the distribution patterns of hot and cold spots at both global and local scales.

2.2.1. Land-Use Transfer Matrix

As a classical statistical model for characterizing the spatiotemporal evolution of land cover patterns, the land-use transfer matrix can systematically decode the bidirectional conversion mechanisms and areal throughput dynamics of various land-cover types between the initial and terminal observation points within a specific time span. The mathematical formulation of the transfer matrix is as follows:

$$S_{ij} = \begin{bmatrix} S_{11} & S_{12} & \cdots & S_{1n} \\ S_{21} & S_{22} & \cdots & S_{2n} \\ \cdots & \cdots & \cdots & \cdots \\ S_{n1} & S_{n2} & \cdots & S_{nn} \end{bmatrix} \quad (1)$$

where S denotes the spatial area; n indicates the algebraic order of the transfer matrix (i.e., the total number of land-use types); i and j represent the land-cover types at the beginning and the end of the study period, respectively; and S_{ij} represents the area converted from the initial land-use type i

to the terminal land-use type *j* during the specific time span.

2.2.2. Grid Cell Spatial Measurement Method

Essentially, the grid cell spatial measurement method discretizes and partitions the inherently continuous and irregular geographic space into standardized rectangular (or square) vector grid cells. Because the change patches extracted by deep learning models are typically fragmented and irregular polygons, direct comparisons from a global perspective struggle to capture local spatial variations adequately. Therefore, by defining a uniform "spatial scale" (e.g., a 1 km × 1 km grid), this method transforms disordered geometric shapes into an ordered matrix arrangement, thereby establishing a strictly consistent and standardized underlying reference frame for all spatial features.

When measuring the spatial evolution of cropland non-agriculturalization, the grid method can accurately calculate the absolute area and relative proportion of land-use conversion occurring within each independent grid cell. This facilitates the construction of a spatial distribution map of the cropland non-agriculturalization rate across the entire study area, thereby achieving a quantitative characterization of the conversion patterns from cropland to non-agricultural uses.

2.2.3. Spatial Autocorrelation Analysis

The Global Moran's I index is employed to measure the overall spatial correlation patterns and agglomeration tendencies of cropland non-agriculturalization across the entire study area. The mathematical formulation is expressed as follows:

$$I = \frac{n\sum_{i=1}^{n}\sum_{j=1}^{n} w_{ij}(x_i-\bar{x})(x_j-\bar{x})}{\left(\sum_{i=1}^{n}\sum_{j=1}^{n} w_{ij}\right)\sum_{i=1}^{n}(x_i-\bar{x})^2} \tag{2}$$

where *I* represents the Global Moran's I index, with values ranging from [-1, 1]. An $I > 0$ indicates positive spatial autocorrelation (i.e., the spatial clustering of high values with high values, and low values with low values). An $I < 0$ indicates negative spatial autocorrelation (i.e., high values adjacent to low values). When *I* approaches *0*, it suggests that the non-agriculturalization phenomenon is completely randomly distributed in space. *N* denotes the total number of spatial units within the study area (e.g., standard grids, administrative villages, or townships). x_i and x_j are the observed values of spatial units *i* and *j*, respectively (i.e., the cropland non-agriculturalization rate within the grid). $\bar{x}$ is the mathematical expectation (global mean) of the observed values across all spatial units. w_{ij} represents the elements in the spatial weight matrix, which are used to define the adjacency relationships or the intensity of spatial interaction between spatial units *i* and *j*.

Although the global index can reflect the overall trend, it may mask local spatial imbalances. Therefore, it is typically necessary to introduce local spatial association indicators to accurately pinpoint the "hot spot" and "cold spot" zones of cropland non-agriculturalization. The mathematical formulation is expressed as follows:

$$I_i = \frac{x_i-\bar{x}}{S^2}\sum_{j=1,j\neq i}^{n} w_{ij}\left(x_j-\bar{x}\right) \tag{3}$$

where the calculation formula for the sample variance S^2 is:

$$S^2 = \frac{1}{n}\sum_{i=1}^{n}(x_i-\bar{x})^2 \tag{4}$$

2.3. Driving Factor Analysis

This study introduces a spatial stratified heterogeneity attribution model (specifically, the factor detector module within the Geographic Detector) to quantitatively analyze the intensity of the spatial coupling response between various driving variables and the non-agriculturalization rate [17]. The core underlying rationale of this model lies in evaluating the impact of the spatial stratified heterogeneity of a single independent variable *X* on the evolution pattern of the dependent variable *Y* (cropland non-agriculturalization rate). The mathematical formulation of its metric, the *q-statistic*, is defined as follows:

$$q = 1 - \frac{\sum_{h=1}^{L} N_h\sigma_h^2}{N\sigma^2} \tag{5}$$

where *L* denotes the number of spatial strata of the driving factor *X* following discretization processing; N_h and *N* represent the total number of grid cells within stratum *h* and the entire study area, respectively; σ_h^2 and σ^2 correspond to the variance of the non-agriculturalization rate in stratum *h* and the entire region, respectively. The value of the *q*-statistic strictly falls within the closed interval [0, 1]. A larger *q-value* indicates a stronger explanatory power of the independent variable *X* (the driving factor) on the dependent variable *Y* (the cropland non-agriculturalization rate).

Furthermore, this study employs the Jenks Natural Breaks classification method to categorize continuous driving factors into 5 to 8 strata, thereby fulfilling the categorical requirements of the Geographic Detector model for input variables.

3. Experiments and Results

Based on the proposed semantic change detection model, MCC-SCNet, the preprocessed test set was fed into the network to obtain the detection results of cropland non-agriculturalization in Zhengzhou City for the consecutive periods of 2021-2022, 2022-2023, 2023-2024, 2024-2025, and the overall period of 2021-2025. Selected localized visualizations are illustrated in Figure 2.

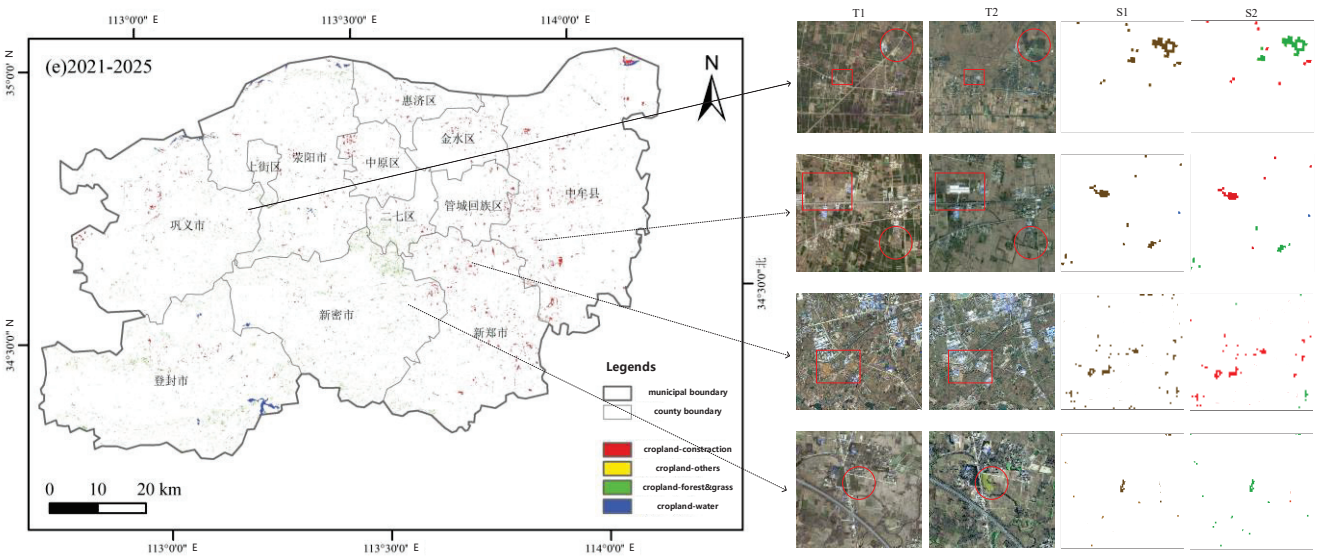

Figure 2. Prediction results of cropland non-agriculturalization in Zhengzhou City from 2021 to 2025 based on MCC-SCNet

From 2021 to 2025, cropland non-agriculturalization in Zhengzhou City exhibited significant characteristics of spatial and typological differentiation. Regarding the conversion types, the conversion from cropland to construction land (red) emerged as the absolute dominant type, reflecting that construction occupation driven by the processes of urbanization and industrialization constitutes the core driver of agricultural land loss. The scales of conversion from cropland to forest and grassland (green), water bodies (blue), and other land uses (yellow) were relatively small, predominantly concentrated in areas undergoing ecological restoration and comprehensive territorial consolidation.

Regarding the spatial pattern, non-agriculturalization patches were highly concentrated in the central urban core and near-suburb regions, such as Zhongmu, Xinzheng, and Xingyang. Conversely, in far-suburb counties and cities, including Gongyi, Dengfeng, and Xinmi, the converted patches were dispersedly distributed, experiencing substantially weaker impacts from urbanization.

3.1. Analysis of Spatiotemporal Characteristics of Cultivated Land Non-agriculturalization

3.1.1. Temporal Characteristics Analysis

Based on the five-period detection results of cultivated land non-agriculturalization, combined with the land-use transfer matrix, the conversion destinations and area statistical information of cultivated land non-agriculturalization were obtained, as shown in Figure 3.

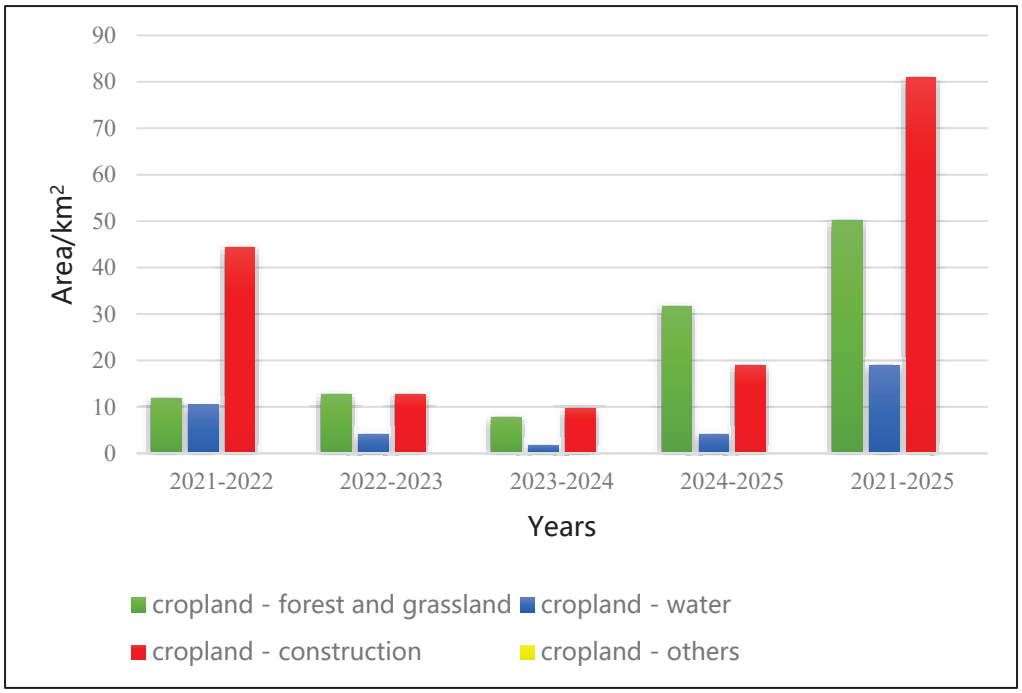

Figure 3. 2021-2025 Zhengzhou city cultivated land non-agriculturalization type and area statistical chart

As Figure 3 intuitively illustrates, over the five-year cumulative changes, construction land occupied an absolute dominant position among all conversion destinations, with its area exceeding 80 km², far surpassing other land-cover types. This reflects that various engineering construction and expansion activities during the rapid urbanization process

constitute the core drivers of cultivated land loss in the study area. Apart from construction land, "forest and grassland" represented the second largest destination for cultivated land outflow, with a five-year cumulative converted area of approximately 50 km². In contrast, the areas of cultivated land converted to "water" and "other" land uses were relatively small.

From the perspective of temporal evolution characteristics, the intensity of cultivated land conversion exhibited an unbalanced fluctuating pattern characterized by "initial intensity, subsequent stabilization, and localized rebound." During the 2021-2022 period, land-cover conversion was most active, with multiple types of non-agriculturalization patches emerging densely. Subsequently, between 2022 and 2024, influenced by the dual impacts of macroeconomic structural adjustments and strict cultivated land-use regulation policies, the expansion trend of non-agriculturalization was significantly curbed. By the 2024-2025 period, potentially driven by the advancement of major local infrastructure projects, the phenomenon of cultivated land occupation by construction land experienced a slight rebound.

3.1.2. Spatial Characteristics Analysis

By interpreting the preprocessed image test set of Zhengzhou City from 2021 to 2025 using the MCC-SCNet model, the spatial distribution information of cultivated land non-agriculturalization was obtained, as illustrated in Figure 4.

From the perspective of spatial distribution, cultivated land non-agriculturalization in Zhengzhou City exhibits significant characteristics of regional gradient differentiation and typological spatial agglomeration, with distinct non-agriculturalization patterns across different functional territories. Specifically, the central urban core and its peripheral areas were the early hot spot zones for cultivated land non-agriculturalization, but they gradually trended toward saturation in the mid-to-late stages of the study period. This region is dominated by the conversion of cultivated land to construction land, with the converted patches mostly exhibiting a fragmented and mosaic-like distribution. This reflects that urban internal development is primarily characterized by stock renewal and edge-infill development, resulting in a gradual contraction in the scale of newly occupied cultivated land.

The near-suburb plains, including Xingyang City, Zhongmu County, and Xinzheng City, constitute the core zone of cultivated land non-agriculturalization in Zhengzhou City. Endowed with flat terrain and superior development conditions, this region has accommodated massive urban new district construction, industrial park establishments, and transportation infrastructure layouts. The conversion of cultivated land to construction land here manifests as large-scale, contiguous expansion, making it the region with the highest intensity and largest scale of non-agriculturalization during the study period. This intensively embodies the rigid occupation of cultivated land driven by rapid urbanization. Conversely, in the far-suburb hilly and mountainous regions, such as Dengfeng City and Xinmi City, the overall intensity of cultivated land non-agriculturalization is relatively low, presenting a scattered, dot-like spatial distribution. The non-agriculturalization types in this region are primarily dominated by conversions to forest land and other land uses, which are closely related to activities such as mine ecological restoration and industrial/mining construction. Cultivated land conversion here is driven more by policy interventions and resource development, exhibiting non-agriculturalization characteristics starkly different from those of the near-suburb plains.

From the perspective of the spatial structure of conversion types, the transition from cultivated land to construction land consistently occupied the absolute dominant position. Spatially, it is highly agglomerated along urban development axes and key development zones, representing the primary manifestation of cultivated land non-agriculturalization in Zhengzhou City. The conversion of cultivated land to forest land is primarily concentrated in the western and southern low-mountain and hilly belts. Conversions to other land uses are mostly distributed in industrial/mining concentration areas and land consolidation regions; although relatively small in overall scale, they exert a non-negligible impact on the cultivated land pattern in localized areas. The conversion of cultivated land to water bodies appears only sporadically along the Yellow River and around reservoirs and wetlands, which is associated with water conservancy engineering construction and aquatic ecological governance, having a limited impact on the city's total volume of cultivated land non-agriculturalization.

Comprehensively, from 2021 to 2025, cultivated land non-agriculturalization in Zhengzhou City presented a spatial gradient pattern characterized by "commencing in the central urban core, highly aggregating in near suburbs, and dispersedly distributing with low intensity in far suburbs." Temporally, it followed an evolutionary trajectory of "sporadic initiation-near-suburb acceleration-global expansion-high-level concentration." The cultivated land non-agriculturalization process is highly coupled with the urbanization trajectory, regional functional positioning, and spatial development policies of Zhengzhou City.

3.1.3. Analysis of the Non-agriculturalization Rate

To finely characterize the macroscopic patterns of cultivated land non-agriculturalization in Zhengzhou City, this study calculates the cultivated land non-agriculturalization rate using the grid cell spatial measurement method, thereby analyzing the degree of cultivated land conversion at the grid scale within the study area [17]. Following the calculation methodology outlined in Reference [17], and striking a balance between the global spatial scale and computational overhead, this study sets the standardized vector fishnet at 1 km × 1 km. Subsequently, the relative proportion of the non-agriculturalized area within each independent grid cell is systematically calculated. This outputs the spatial distribution of the cultivated land non-agriculturalization rate covering four consecutive periods (2021-2022, 2022-2023, 2023-2024, and 2024-2025), as well as the overall temporal evolution from 2021 to 2025, as detailed in Figure 5.

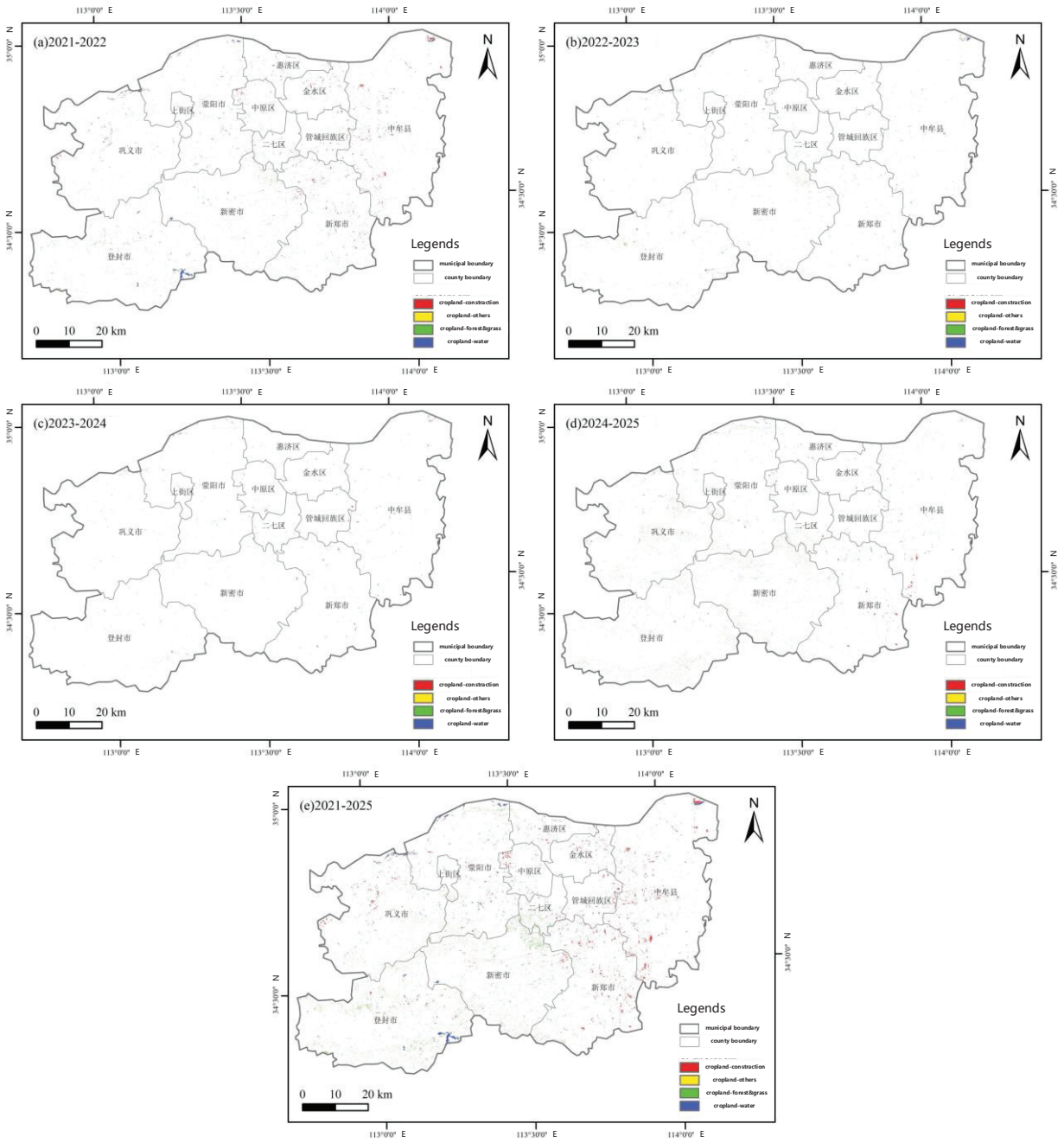

Figure 4. Spatial distribution of cultivated land non-agriculturalization in Zhengzhou City from 2021 to 2025

In Figure 5, each sub-figure employs the Jenks Natural Breaks classification method to divide the grid-based cultivated land non-agriculturalization rate into five levels. The colors range from light yellow to dark red, representing non-agriculturalization rates from low to high: light yellow indicates low-rate zones where cultivated land remains fundamentally stable with weak non-agriculturalization activities; light orange represents medium-low-rate zones with sporadic cultivated land conversion; orange denotes medium-rate zones with relatively active conversion activities; dark orange signifies medium-high-rate zones with a high conversion intensity; dark red represents high-rate zones with significant conversion intensity, serving as the non-agriculturalization hot-spot grids during the study period. The differences in classification thresholds across different periods reflect a phased upward trend in the overall non-agriculturalization level during the study period.

From the perspective of the grid-scale spatial pattern, the cultivated land non-agriculturalization intensity in Zhengzhou City from 2021 to 2025 exhibited significant spatiotemporal differentiation characteristics. In the temporal dimension, the non-agriculturalization rate showed an overall continuous upward trend throughout the study period. It sequentially experienced a global low-intensity stage (2021-2022), an agglomeration stage around the central urban core (2022-2023), a global multi-point expansion stage (2023-2024), and a high-intensity contiguous development stage in the near-suburb plains (2024-2025). The non-agriculturalization intensity gradually escalated over time, progressing from isolated points to extensive surfaces, and from localized areas to the global scale.

In the spatial dimension, the non-agriculturalization rate presented a distinct "core-periphery" gradient pattern. Specifically, the periphery of the central urban core and the near-suburb plains of Zhongmu, Xingyang, and Xinzheng constituted the high-intensity core zones of non-agriculturalization, forming contiguous high-value belts extending along the urban development axes. Conversely, the

far-suburb hilly and mountainous regions, such as Dengfeng and Xinmi, were dominated by medium-low non-agriculturalization rates, where cultivated land generally remained stable.

A comprehensive synthesis of the multi-period spatial distributions of the non-agriculturalization rate further indicates that the near-suburb plain region is the primary spatial carrier for cultivated land non-agriculturalization in Zhengzhou City. Its high-intensity non-agriculturalization is highly coupled with the spatial layout of urban construction and industrial development. Meanwhile, restricted by topographic conditions and ecological functions, the far-suburb hilly regions exhibited a lower cumulative non-agriculturalization intensity, facing relatively lighter pressures regarding cultivated land protection.

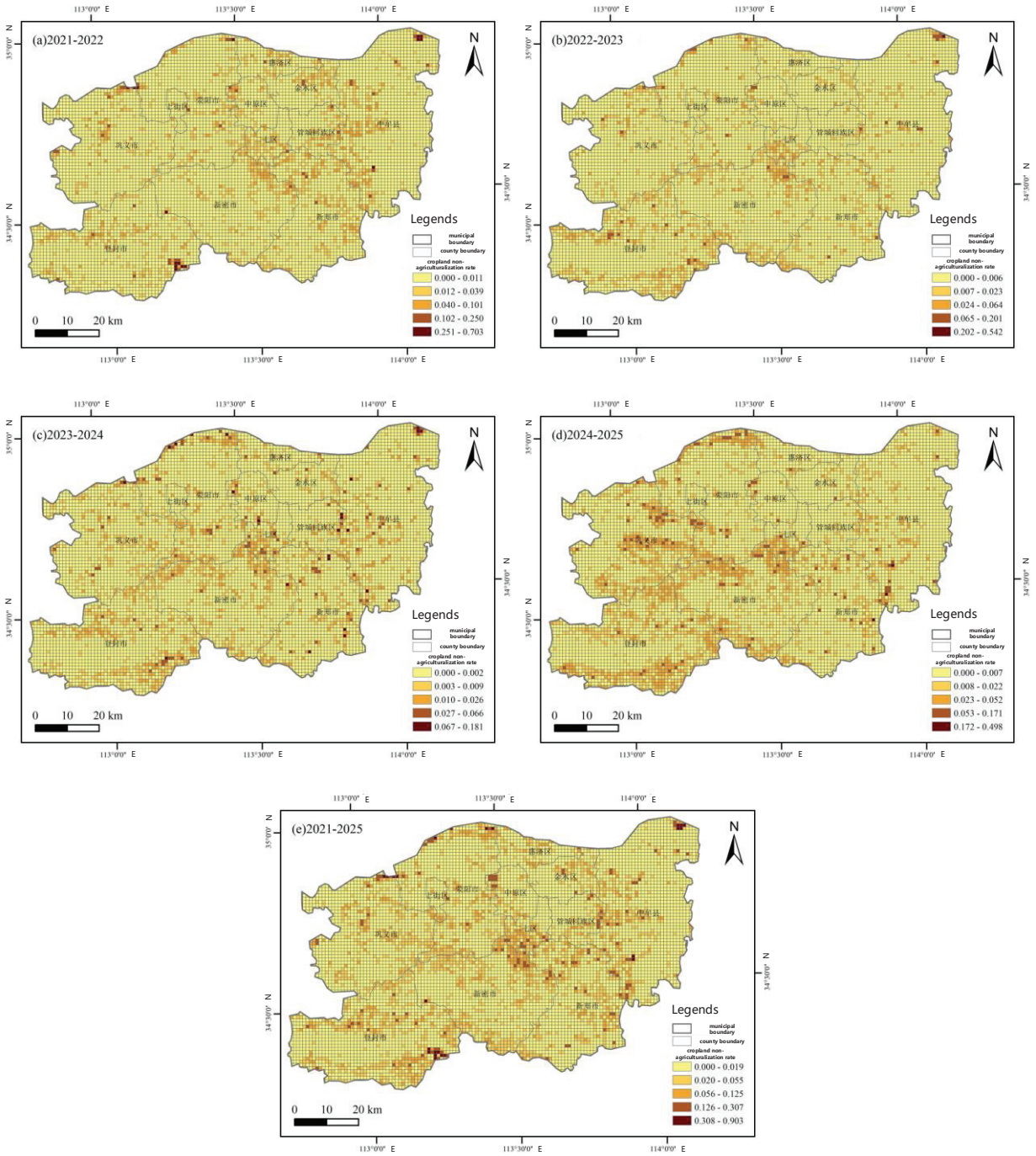

Figure 5. Grid-based spatial distribution of the cultivated land non-agriculturalization rate in Zhengzhou City from 2021 to 2025

3.1.4. Cold and Hot Spot Analysis of Cultivated Land Non-agriculturalization

To further explore the spatial interaction relationships and overall agglomeration patterns of cultivated land non-agriculturalization in Zhengzhou City, the Global Moran's I indices for the study area across different periods were calculated using Equation (2), as presented in Table 1.

Statistical results demonstrate that across all observation periods, the *p-values* were consistently less than *0.001*, and the Global Moran's I indices were all positive. This reveals that the high-value areas of cultivated land non-agriculturalization in Zhengzhou City are adjacent to other high-value areas, and low-value areas are clustered with other low-value areas, collectively presenting a highly polarized

spatial distribution pattern. From the perspective of the temporal evolution trajectory, the degree of global agglomeration exhibited an evolutionary pattern characterized by an "initial increase, subsequent decline, and final rebound."

Table 1. Global Moran's I indices of cultivated land non-agriculturalization in Zhengzhou City across different periods

Years	2021-2022	2022-2023	2023-2024	2024-2025	2021-2025
Moran's I	0.32	0.221	0.214	0.315	0.363
Z	40.008	28.344	26.622	39.342	44.998

Because the Global Moran's I index can only reveal the overall clustering tendency, it struggles to finely characterize the specific distribution patterns of high or low values within localized areas. Therefore, this study introduced the *Getis-Ord* G_i spatial statistics index (Equation 3) to conduct a cold and hot spot spatial analysis on the non-agriculturalization rate grids of Zhengzhou City for the periods of 2021-2022, 2022-2023, 2023-2024, 2024-2025, and the overall 2021-2025 period, as illustrated in Figure 6.

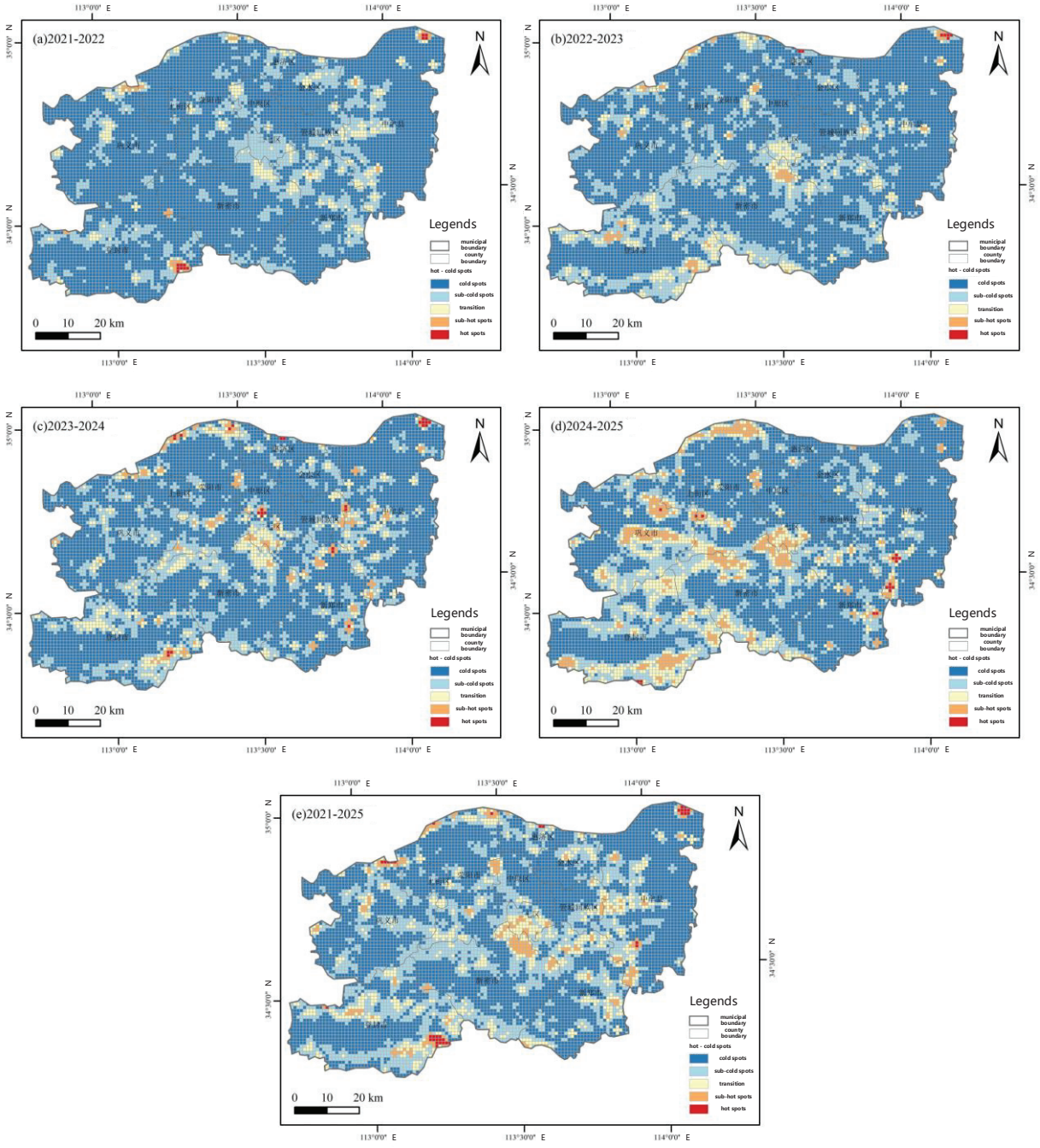

Figure 6. Spatial distribution of cold and hot spots of cultivated land non-agriculturalization in Zhengzhou City from 2021 to 2025

In Figure 6, the local spatial clustering characteristics of cultivated land non-agriculturalization are divided into five categories. The colors, transitioning from blue to red, represent the non-agriculturalization clustering levels from low to high: Cold spot zone (dark blue): Indicates low-value clustering areas of non-agriculturalization, where the surrounding non-agriculturalization rates are generally low, presenting significant "low-low" clustering characteristics in space. This represents a fundamentally stable zone for cultivated land. Sub-cold spot zone (light blue): Represents a transitional type of low-value clustering. The surrounding non-agriculturalization level is generally low but exhibits certain fluctuations, and its spatial clustering significance is weaker than that of the cold spot zone. Transition zone (light yellow): Denotes an area where the spatial clustering of non-agriculturalization is not statistically significant. There is no obvious high-value or low-value clustering, and the non-agriculturalization process is dominated by local spatial factors. Sub-hot spot zone (light orange): Represents a transitional type of high-value clustering. The surrounding non-agriculturalization level is generally high, serving as a potential area evolving toward a hot spot zone. Hot spot zone (red): Indicates high-value clustering areas of non-agriculturalization, where the surrounding non-agriculturalization rates are generally high, presenting significant "high-high" clustering characteristics in space. This constitutes the core agglomeration zone of cultivated land non-agriculturalization.

The results of the local spatial autocorrelation analysis indicate that the spatial clustering characteristics of cultivated land non-agriculturalization in Zhengzhou City underwent significant changes over time from 2021 to 2025. In the temporal dimension, the cold and hot spot pattern experienced an evolutionary process of "global cold spot dominance-emergence of sporadic hot spots-multi-center sub-hot spot expansion-formation of contiguous hot spots in near suburbs." The high-value agglomeration centers of non-agriculturalization gradually evolved from isolated dot-like distributions to contiguous agglomeration belts in the near-suburb plains. Specifically, between 2021 and 2024, the hot spot zones were mostly distributed as scattered points around the periphery of the central urban core; however, by the 2024-2025 period (Fig. 6(d)), large-scale contiguous sub-hot spot and hot spot agglomeration belts emerged in the central-western region (Xinmi City). Considering the five-year cumulative spatial pattern (Fig. 6(e)), the eastern (Zhongmu County) and southern (Xinzheng City) regions constituted the core hot spot expansion zones of cultivated land non-agriculturalization within the Zhengzhou municipal area.

In the spatial dimension, the study area presented a distinct "core-periphery" agglomeration pattern. The near-suburb plains, with the periphery of the central urban core and the northern parts of Zhongmu County, Xingyang City, and Xinzheng City as the core, served as the concentrated distribution areas for non-agriculturalization hot spots and sub-hot spots, forming a "high-high" clustering non-agriculturalization core belt. Conversely, the hilly and mountainous regions in western Gongyi City, Dengfeng City, and Xinmi City persistently remained in cold spot and sub-cold spot zones, featuring low non-agriculturalization levels and significant spatial clustering. This spatial distribution pattern further corroborates the evolution patterns analyzed previously.

In summary, the cold and hot spot pattern of cultivated land non-agriculturalization is highly coupled with regional topographic conditions, urban development directions, and land-use regulation policies. The near-suburb plains are not only the primary regions for the high-value agglomeration of non-agriculturalization but also the priority areas for future cultivated land protection and regulation.

3.2. Analysis of the Driving Mechanisms of Cultivated Land Non-agriculturalization

To quantitatively reveal the core driving forces behind the spatiotemporal evolution of cultivated land non-agriculturalization in Zhengzhou City, this study employed the Geographic Detector model (Equation 5) to calculate the explanatory power (*q-value*) of 11 selected indicators on the non-agriculturalization rate within the study area, as presented in Table 2. These 11 indicators encompass location factors (distance to roads X_1, distance to railways X_2, distance to urban centers X_3, distance to water systems X_4), natural factors (elevation X_5, slope X_6, aspect X_7), and social factors (growth rate of resident population X_8, growth rate of population urbanization X_9, growth rate of the primary industry GDP index X_{10}, and growth rate of regional GDP X_{11}).

The *q-value* in the Geographic Detector strictly ranges within the closed interval [0, 1]. A larger *q-value* indicates a stronger explanatory power of the driving factor on the cultivated land non-agriculturalization rate, and vice versa. Based on the temporal variations and comprehensive rankings of the *q-values*, the detailed analysis is conducted from three aspects: the overall pattern, temporal evolution, and key factors, as detailed below.

Table 2. Global Moran's I indices of cultivated land non-agriculturalization in Zhengzhou City across different periods

Indices	2021-2022		2022-2023		2023-2024		2024-2025		2021-2025	
	q	No.	*q*	No.	*q*	No.	*q*	No.	*q*	No.
X_1	0.188	8	0.278	6	0.212	7	0.343	6	0.125	10
X_2	0.27	4	0.63	2	0.371	4	0.435	5	0.524	1
X_3	0.234	7	0.331	4	0.101	10	0.243	10	0.261	8
X_4	0.253	6	0.212	7	0.118	9	0.63	3	0.305	4
X_5	0.266	5	0.343	3	0.449	2	0.849	2	0.292	5
X_6	0.492	2	0.323	5	0.449	3	0.853	1	0.292	6
X_7	0.328	3	0.166	10	0.507	1	0.189	11	0.198	9
X_8	0.141	10	0.184	9	0.296	5	0.526	4	0.289	7
X_9	0.15	9	0.085	11	0.229	6	0.305	8	0.124	11
X_{10}	0.553	1	0.646	1	0.043	11	0.341	7	0.436	2
X_{11}	0.136	11	0.212	8	0.154	8	0.275	9	0.324	3

3.2.1. Global Driving Characteristics

From the overall perspective of the 2021-2025 results, the spatial evolution of cultivated land non-agriculturalization in Zhengzhou City exhibits distinct characteristics that are "transportation location-dominated, industrial economy-supported, and topographic condition-constrained," with significant variations in influence intensity among different factor categories.

Specifically, the *q-value* of the distance to railways (X_2) is the highest among all factors (*0.524*), demonstrating that transportation location-particularly the spatial distribution of railway hubs-is the core influential factor driving cultivated land non-agriculturalization, making zones along railway lines high-incidence belts for non-agriculturalization. As an industrial economy factor, the growth rate of the primary industry GDP index (X_{10}, $q = 0.436$, ranked second) reflects that agricultural structural adjustment and the conversion of agricultural land to non-agricultural uses constitute the core economic driver. The regional GDP growth rate (X_{11}) represents the macro-level economic development of the region; its high explanatory power indicates that infrastructure construction and urban expansion fueled by economic growth serve as major impulses for non-agriculturalization. Regarding natural factors, elevation (X_5) and slope (X_6) exhibit similar *q-values* and rank prominently (both at *0.292*), which indicates that topographic conditions act as rigid physical constraints on the spatial layout of non-agriculturalization. Low-elevation and gentle-slope plain areas are preferentially selected for construction and development, thus showing substantial explanatory power for the non-agriculturalization rate. Conversely, the growth rate of the resident population (X_8) and the population urbanization growth rate (X_9) show weaker explanatory power. This suggests that population size expansion and increasing urbanization rates exert limited direct driving effects, confirming that non-agriculturalization is not a simplistic population-driven urbanization process but rather a structural transformation centered on industry and transportation. Aspect (X_7) exhibits the weakest explanatory power, playing only a phased role in specific periods and exercising a limited impact on the overall process.

3.2.2. Temporal Dynamic Evolution

Based on the temporal variations in *q-values* across the four consecutive periods, the driving factors of cultivated land non-agriculturalization in Zhengzhou City present clear phased evolutionary characteristics, with core driving factors differing substantially across different periods.

2021-2022: The core driving factor during this period was the growth rate of the primary industry GDP index (X_{10}, $q = 0.553$, ranked first). This underscores that agricultural structural adjustment served as the core momentum at this stage, and the transition of agricultural land to secondary and tertiary industrial uses was the primary cause of cultivated land reduction. Socioeconomic factors such as regional GDP growth rate, population growth rate, and urbanization growth rate ranked lower, indicating that the socioeconomic driving force was relatively weak initially.

2022-2023: The core driving factor remained the growth rate of the primary industry GDP index (X_{10}, $q = 0.646$, ranked first). Its *q-value* increased compared to the previous period, indicating a continuously strengthening industrial driving effect. The *q-value* for the distance to railways X_2 reached *0.63* (No.2), revealing that development and construction along railway lines became a critical contributor to non-agriculturalization, marking a comprehensive rise in the catalytic role of transportation location. The elevation factor (X_5) had a *q-value* of *0.343* (No.3), demonstrating that topographic constraints remained pronounced.

2023-2024: During this period, topography emerged as the core driver of non-agriculturalization, with the *q-values* for both elevation (X_5) and slope (X_6) reaching *0.449*. This indicates that the spatial layout of non-agriculturalization was heavily constrained by topographic conditions, forcing development activities to concentrate in areas with optimal terrain. Concurrently, the *q-value* for the primary industry GDP index plummeted to *0.043*, signifying a phased invalidation of the industrial driving effect and reflecting a significant weakening of agricultural structural adjustments on the non-agriculturalization process. The distance to railways (X_2) maintained a medium-high influence ($q = 0.371$), indicating a persistent catalytic role for transportation location.

2024-2025: Topographic factors consistently maintained their position as the core drivers. The *q-values* for both slope (X_6) and elevation (X_5) surpassed *0.8,* demonstrating that as cultivable land resources suitable for development became increasingly scarce in Zhengzhou City, the spatial selection for non-agriculturalization depended critically on topographic conditions, making high-quality cultivated land with low slope and low elevation the primary targets for development occupation. Population growth rate (X_8, $q = 0.526$) and distance to railways (X_2, $q = 0.435$) sustained medium-high influences, indicating the persistent driving roles of transportation and population. Factors such as the primary industry GDP index and the urbanization growth rate ranked lower, suggesting that the direct driving effects of industry and urbanization were relatively weak at this stage.

3.2.3. Key Factors Analysis

Within the transportation location factors, the comprehensive *q-value* of the distance to railways (X_2, *0.524*) is far higher than that of the distance to roads (X_1, *0.125*). From the perspective of temporal variation, the *q-value* for the distance to railways surged drastically during 2022-2023 and consistently maintained a high influence thereafter, indicating that the radiating effect of railway hubs served as a major engine for cultivated land non-agriculturalization in Zhengzhou City.

Among the industrial economy factors, the growth rate of the primary industry GDP index (X_{10}) is the central driving force. Temporally, this factor consistently ranked first during 2021-2023, acting as the absolute dominant force in the early stages of non-agriculturalization, and only experienced a phased decline during 2023-2024. Overall, it presented strong driving characteristics, which highly corroborates the "fast-slow-rebound" spatiotemporal distribution characteristics of cultivated land non-agriculturalization in Zhengzhou City. As a representative of the macroeconomy, the regional GDP growth rate (X_{11}) ranked third comprehensively, acting as a stable, medium-strong driving factor. This reflects that infrastructure construction and urban expansion driven by economic growth provide continuous momentum for cultivated land non-agriculturalization.

Among the topographic factors, elevation (X_5) and slope (X_6) are the core physical constraints. Zhengzhou City is situated in the transition zone from the western Henan mountainous region to the eastern Henan plain, and

topographic conditions directly dictate land development suitability. Low-elevation and gentle-slope plain regions are the priority choices for construction and development, whereas high-altitude and steep-slope areas face severe development cost limitations, resulting in a low degree of non-agriculturalization. Consequently, topographic factors provide a highly robust explanation for the spatial stratified heterogeneity of the cultivated land non-agriculturalization rate.

4. Conclusions

This study utilizes the MCC-SCNet semantic change detection model to conduct a long time-series interpretation and analysis of GF-2 imagery of Zhengzhou City from 2021 to 2025. By comprehensively integrating cultivated land conversion area statistics, the spatial distribution of non-agriculturalization, and the grid-based non-agriculturalization rate, this study systematically reveals the spatiotemporal distribution characteristics and evolution patterns of cultivated land non-agriculturalization in this region. The main conclusions are drawn as follows:

(1) In peri-urban areas characterized by a high degree of fragmentation and complex land-cover categories, the multi-channel complementary semantic change detection network (MCC-SCNet) constructed in this study demonstrates exceptional robustness. Validated through a multi-class confusion matrix and cultivated land area transfer accuracy assessment, the model effectively suppresses "pseudo-changes" caused by illumination and phenology, providing high-fidelity foundational data support for subsequent large-scale, long time-series spatial analyses.

(2) During the study period, the intensity of cultivated land conversion in Zhengzhou City transitioned from an initial "intense outbreak" to a subsequent "overall stabilization." Grid-based measurements and exploratory spatial data analysis indicate that the non-agriculturalization evolution is by no means a homogeneous spatial diffusion. Hot spot zones are highly agglomerated around the periphery of the central urban core, as well as in eastern Zhongmu County and southern Xinzheng City. This presents typical characteristics of "core-periphery" gradient attenuation and "axial-belt" expansion along main traffic arteries, constituting the spatial main axis of Zhengzhou City's "eastward expansion and southward extension." Constrained by topographic factors such as elevation and slope, the southwestern part of the study area (most of Dengfeng City) has persistently remained a stable non-agriculturalization cold spot zone, fulfilling a critical regional ecological barrier function.

(3) The Geographic Detector results reveal that cultivated land non-agriculturalization in Zhengzhou City is the result of the combined effects of the natural environment and human activities. The spatial evolution of non-agriculturalization exhibits distinct characteristics that are "transportation location-dominated, industrial economy-supported, and topographic condition-constrained." Natural geographic elements (e.g., elevation) constitute the underlying spatial constraints for non-agriculturalization expansion; socioeconomic elements (e.g., GDP, urbanization rate) form the driving engines for non-agriculturalization; while the extension of transportation networks and regional development strategies precisely guide the evolution of non-agriculturalization hot spots.

In summary, the long time-series data acquired based on deep learning interpretation can quantitatively characterize the spatiotemporal evolution patterns of cultivated land non-agriculturalization. This provides a scientific data foundation and technical support for territorial spatial regulation and cultivated land redline early warning.

References

[1] Cai, Y., & Zhang, L. (2004). Analysis on the evolution characteristics of cultivated land non-agriculturalization in Wuhan city in recent years. *China Population, Resources and Environment*, *14*(6), 115-119.

[2] Zhong, T., Huang, X., Zhang, X., et al. (2011). Temporal and spatial variability of agricultural land loss in relation to policy and accessibility in a low hilly region of southeast China. *Land Use Policy*, *28*(4), 762-769. https://doi.org/10.1016/j.landusepol.2011.03.004

[3] Fan, H., Liu, W., & Wu, Z. (2014). Spatial-temporal changes of arable land non-agriculture at county scale in Henan province—From the perspective of hydrologic basin. *Bulletin of Soil and Water Conservation*, *34*(1), 207-213.

[4] Zhang, X., Xie, X., & Zhang, A. (2014). Spatial unbalanced development and diffusion route of farmland conversion in Wuhan city. *Journal of Natural Resources*, *29*(10), 1649-1659.

[5] Ma, C., Zhao, L., & Ke, X. (2016). Temporal spatial variation of the pressure of cropland non-agriculturalization in Hubei province. *Resources and Environment in the Yangtze Basin*, *25*(1), 71-78.

[6] Qu, S., Liu, Y., Yin, Z., et al. (2020). Spatial pattern of cultivated land change in Fujian Province from 1990 to 2015. *Chinese Journal of Eco-Agriculture*, *28*(4), 587-598. https://doi.org/10.13930/j.cnki.cjea.190823

[7] Liu, S., Wang, J., Lin, S., et al. (2022). The spatial features and migration path of cultivated land non-agriculturalization in the border areas of Guangxi Zhuang Autonomous Region. *Chinese Journal of Agricultural Resources and Regional Planning*, *43*(10), 162-173.

[8] Huang, T., & Xu, J. (2023). The characteristics, causes and countermeasures of spatial-temporal evolution of Guangxi cultivated land de-agriculturalization in the past 40 years. *Chinese Journal of Agricultural Resources and Regional Planning*, 1-12.

[9] Li, X., Tian, D., & Tan, J. (2022). Spatio-temporal pattern evolution and influencing factors of cultivated land non-agriculturalization in Yan'an city. *Bulletin of Soil and Water Conservation*, *42*(4), 330-337.

[10] Wu, H., Tian, X., & Zhang, L. (2023). Spatio-temporal dynamics characteristic and diffusion trend of cultivated land conversion in Anhui province in recent 40 years. *Chinese Journal of Agricultural Resources and Regional Planning*, 1-11.

[11] Li, X., Zhou, Y., Liu, Y., et al. (2025). Spatiotemporal characteristics and evolution of non-agricultural farmland in Yunnan province. *Chinese Journal of Agricultural Resources and Regional Planning*, *46*(5), 212-223.

[12] Liu, H., Wang, H., Jin, Z., et al. (2024). Spatial and temporal evolution characteristics and driving mechanism of cultivated land conversion in Lower Liaohe River Plain. *Chinese Journal of Eco-Agriculture*, *32*(8), 1420-1431. https://doi.org/10.13930/j.cnki.cjea.240117

[13] Liu, F., Wu, X., & Guo, Z. (2024). Spatio-temporal evolution characteristics and dynamic trends of cultivated land conversion in county: A case study of Anhui province. *Journal of Northeast Agricultural University*, *55*(4), 50-61.

[14] Yu, Q., & Wang, H. (2024). Analysis on temporal and spatial evolution characteristics of farmland conversion in Henan

province. *Scientific and Technological Management of Land and Resources*, *41*(2), 50-61.

[15] Kang, Q., Sun, P., Yang, L., et al. (2023). Study on the spatiotemporal evolution characteristics of cultivated land non-agriculturalization: A case study of Danjiangkou city. *Agriculture and Technology*, *43*(7), 19-22.

[16] Li, X., Lei, S., Li, K., et al. (2026). Analysis of the spatiotemporal evolution characteristics of cultivated land non-agriculturalization in the Jialing River Basin (1980-2020). *Journal of Changjiang River Scientific Research Institute*, 1-9.

[17] Ding, S., Li, M., Wang, X., et al. (2022). The use of time series remote sensing data to analyze the characteristics of non-agriculture farmland and their driving factors in Fuzhou. *Remote Sensing Technology and Application*, *37*(3), 550-563.

[18] Chen, M., & Jiang, W. (2025). SCDVit: Semantic change detection based on SAM-ViT and semantic consistency. *IEEE Journal of Selected Topics in Applied Earth Observations and Remote Sensing*, 2269-2282. https://doi.org/10.1109/JSTARS.2025.3479628

[19] Guo, L., Chen, X., Wang, A., et al. (2026). Multi-scenario simulation of land use and ecosystem service value valuation based on intPLUS model: A case study of resource-based cities in Henan province. *Environmental Science & Technology*, 1-15.

[20] Wei, Y., Wei, F., & Tong, X. (2023). Characterization and attribution identification of “Non-grain” cultivated land in rocky desertification areas in Guangxi. *Resource Development & Market*, *39*(1), 9-15